# A High-Concentration Programmable Solar Simulator for Testing Multi-Junction Concentrator Photovoltaics

Tasshi Dennis<sup>1</sup>, Brent Fisher<sup>2</sup>, Matt Meitl<sup>2</sup>, and John Wilson<sup>2</sup>

<sup>1</sup>National Institute of Standards and Technology, Boulder, CO 80305, USA; <sup>2</sup>Semprius, Inc., Durham, NC 27713, USA

Abstract — We describe the design and operation of a spectrally programmable solar simulator capable of being concentrated to very high irradiance for the testing of multijunction concentrator solar cells. The simulator utilizes a spatially coherent, super-continuum laser as the light source and a hybrid pair of prism-based spectrometers with spatial light modulators to precisely control the spectrum. Spectra are presented which simulate scaled versions of the AM 1.5 solar reference spectrum, correct for spectral mismatch, and model attenuation from increasing air-mass. The simulation of attenuated spectra may be used to study conditions representative of changes in location, weather, time of day, and time of year. We used the programmable simulator to test a multi-junction solar cell at up to 138 suns. We used a static, non-programmable version of the simulator to test the same cell at well over 500 suns. Technical improvements which would achieve substantial increases in irradiance and/or cell illumination area are described.

Index Terms — concentrator photovoltaic, multijunction solar cell, quantum efficiency, solar simulation, spatial light modulator, spectral mismatch, super-continuum laser

Work of an agency of the US government; not subject to copyright.

# I. INTRODUCTION

Measuring the optical and electrical properties of a photovoltaic device or material constitutes a fundamental characterization which is critical to increasing efficiency, improving reliability, and reducing overall solar-cell cost. Such measurements must be made with high accuracy under controlled conditions using an illumination source, or solar simulator, which can be carefully controlled spectrally, spatially, and temporally. Traditionally, the laboratory light sources used for solar-cell testing have included broadband lamps [1], lasers [2], and LEDs [3]. Significant drawbacks exist for each of these sources when used in various measurement scenarios. Arc lamps, for example, can provide a powerful and broad spectrum, but are difficult to spectrally alter for the light biasing of multi-junction solar cells [4] and the modeling of air-mass variations [5]. Lasers are powerful and easy to concentrate, but have unrealistically narrow spectra [2]. LEDs are broader spectrally than lasers but must be configured into interleaved arrays to provide better coverage of the solar spectrum [3]. Lamps and LEDs both radiate into large solid angles, making them difficult to concentrate or alter spectrally with beam optics.

The super-continuum laser is a high-power, broadband light source with the potential to provide vastly improved optical excitation for photovoltaic materials and devices. Unlike a flashed xenon arc lamp, the super-continuum laser is rapidly pulsed at repetition rates up to 80 MHz, resulting in a quasicontinuous beam of light. This novel source offers spectral coverage from the short-wavelength blue out to the infrared, with tens of watts of optical power in a single spatial mode. Previously, NIST has shown that this source can be spectrally shaped efficiently, and appears sun-like to a variety of photovoltaic materials [6]. NIST has also demonstrated that the novel simulator can be focused to a micrometer-scale spot and used for spatially selective, full-spectrum, optical beam induced current [6].

In this work, we report on the full-area illumination of a multi-junction, concentrator solar cell at irradiance levels up to and beyond 500 suns. The design and operation of a hybrid, programmable spectral shaper utilizing two types of spatial light modulators is described. Efficiency measurements for the concentrator cell are presented, including those for illumination conditions which model different atmospheric airmass (AM) representing changes in location, weather, time of day, and time of year.

### II. SIMULATOR DESIGN AND OPERATION

The experimental apparatus used to create the concentrated solar simulator is illustrated in Fig. 1. A commercial supercontinuum laser having more than 7 watts of emission with a spectrum which spans from below 450 nm to beyond 2200 nm

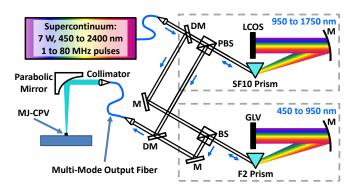


Fig. 1. The programmable concentrator solar simulator apparatus is shown. M: collimation and steering mirrors; DM: dichroic mirror; BS: beam splitter; PBS: polarization beam splitter; GLV: grating light valve; LCOS: liquid crystal on silicon; MJ-CPV: multi-junction concentrator photovoltaic.

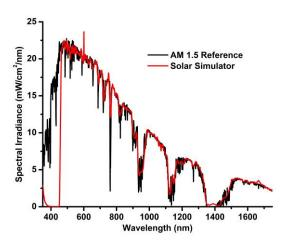


Fig. 2. The simulator spectrum matched to a scaled AM 1.5 reference is shown, resulting in an irradiance of about 138 suns.

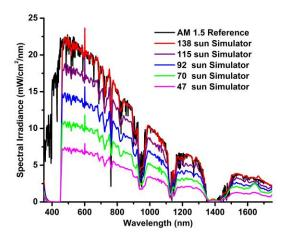


Fig. 3. The simulator spectrum was shaped to scaled AM 1.5 spectra, resulting in irradiances between 47 suns and 138 suns.

was used. In previous work, a liquid-crystal-on-silicon spatial light modulator (LCOS-SLM) was used to actively shape the entire spectrum of the super-continuum laser [7]. In this work, a micro-electro-mechanical (MEMS) device, known as a grating light valve spatial light modulator (GLV-SLM), was added to spectrally shape the short wavelength spectrum. Utilizing this type of SLM device achieves higher optical throughput, with higher efficiency, higher damage threshold (> 10 kW/cm<sup>2</sup>), lower absorption, and low polarization dependence. As shown in Fig. 1, the 12 mm diameter collimated beam of the super-continuum laser was passed through a dichroic beam splitter, which divided the light spectrally above and below 950 nm. The spectrum below 950 nm was controlled by the GLV-SLM, which is a linear array device with 1088 pixels that operates as a steerable diffraction grating [8]. Spectral components incident on the GLV from a prism made of Schott F2 glass [9] were attenuated by steering them out of the beam which reflected back through the prism and out of the short wavelength spectral shaper. The spectrum above 950 nm was controlled by an LCOS-SLM having a 512 x 512 array of pixels, and operated as a polarization diversity switch. As shown, the incident light passed through a polarization beam splitter (PBS) before being dispersed by a prism made of Schott SF10 glass [9]. The LCOS-SLM selectively rotates the polarization state of the reflected spectrum, such that it reflects off the PBS and out of the long wavelength spectral shaper. Light from the two shapers was combined with a second dichroic beam splitter and collected into a multimode fiber with a 200  $\mu m$  core.

Accurate spectral shaping was achieved by operating a closed loop between the voltage patterns driving the SLMs and a spectrometer measuring the output spectrum of the simulator. Because of nonlinearities in the response of our optical system, an iterative approach was used to obtain the optimum voltage patterns which minimized the difference between the target and measured spectra.

An off-axis parabolic mirror with a 152 mm focal length was used to concentrate the light from the simulator, generating a focused beam of broadband light with a measured diameter of 1.0 mm. The ease with which the output of the simulator was concentrated was a direct result of the spatial coherence of the super-continuum laser. Propagation through the step-index multimode fiber resulted in a focused spot of light with an approximate square-top intensity profile.

## III. CONCENTRATED SIMULATOR PERFORMANCE

Figure 2 presents results of spectrally shaping our simulator to match a scaled AM 1.5 (ASTM G-173-03) solar reference spectrum [10], resulting in a concentrated irradiance of about 138 suns. The programmable simulator was able to accurately replicate many of the detailed spectral features caused by atmospheric absorption. The simulation of the deepest spectral features was limited primarily by the finite wavelength

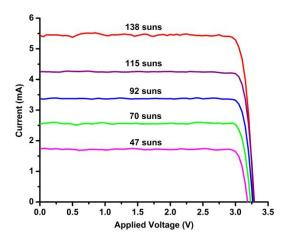


Fig. 4. The measured efficiency of a multi-junction concentrator solar cell is shown illuminated by different levels of irradiance.

resolution of the spectral shaper, which varied with wavelength. The finite amplitude extinction also varied with wavelength at around 3 % and 5 %, limiting the ability to simulate complete atmospheric absorption as seen around 1400 nm. The lack of light below 450 nm is apparent and is the result of the limits of the super-continuum laser spectrum as well as the present optical configuration of the short wavelength spectral shaper. By use of a different prism or a collimation mirror with a shorter focal length, the GLV-SLM would be able to capture more of the short wavelength spectrum. The sharp spike at 575 nm is the result of a faulty pixel in the demonstration-grade, GLV-SLM. Overall, the spectral match from 450 to 1750 is very good and unprecedented relative to conventional solar simulators. Fig. 3 shows additional spectra generated by programming lower levels of irradiance while maintaining the same 1.0 mm beam spot. Fig. 4 presents measured current-voltage efficiency curves obtained from a multi-junction concentrator solar cell

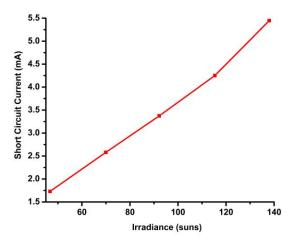


Fig. 5. The measured short-circuit current of a multi-junction solar cell as a function of increasing irradiance.

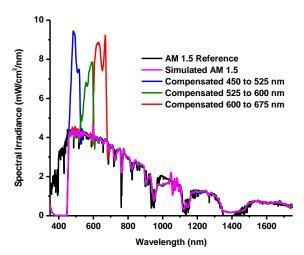


Fig. 6. The generation of several spectra designed to compensate for the spectral mismatch below 450 nm are shown.

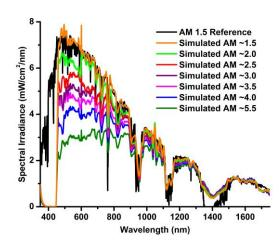


Fig. 7. Spectra which model attenuation from increasing air-mass were simulated.

chip that was fully illuminated by our concentrated simulator beam. As expected at these relatively low levels of irradiance, the short circuit current measured at zero applied voltage increases linearly with irradiance, as shown in Fig. 5. The measured currents in Fig. 4 are noisy relative to traditional simulator measurements and this may be caused by optical instability from spectral shaper light reflecting back toward the laser or a constant dither modulation from the LCOS-SLM.

The lack of spectral content below 450 nm is of particular concern for the testing of some multi-junction solar cells. This spectral mismatch error will result in less short-wavelength light incident on the top junction of a solar cell, causing an imbalance and reduction of the total junction current. Fig. 6 presents three different simulator spectra in which narrow spectral bands have been artificially enhanced to maintain a total integrated irradiance nearly equal to the AM 1.5 reference spectrum. The spectrum with compensation in the middle 525 nm to 600 nm band is a little incomplete because of insufficient super-continuum laser power available in that band. However, each of the three spectra resulted in nearly the same proportional increase in short circuit current, to within 6 %.

For the purposes of industry-wide comparison, cell efficiency is reported in response to the AM 1.5 solar reference spectrum. However, to better understand and optimize the overall performance of a solar cell in response to the variations it will experience in service, it would be of value to consider air-mass conditions beyond AM 1.5. Increases in air-mass represent the transmission of the solar irradiance through a longer atmospheric path, which can be used to model conditions representing changes in location, weather, time of day, and time of year.

Our simulator was easily able to realistically mimic irradiance conditions associated with higher air-mass by making use of its spectral programmability. While the Simple Model of the Atmospheric Radiative Transfer of Sunshine (SMARTS) [5] is a sophisticated and established model for

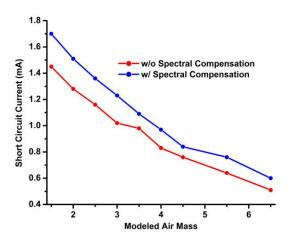


Fig. 8. Increasing air-mass reduces the current of a multi-junction, shown with and without mismatch compensation.

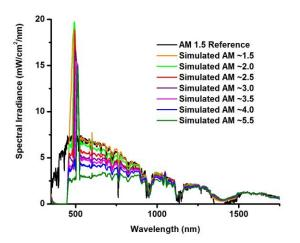


Fig. 9. Spectra which model attenuation from increasing air-mass with additional compensation for spectral mismatch below 450 nm.

irradiance, for the purposes of demonstration we used a simple attenuation model to create progressive air-mass spectra. Our generated spectra presented in Fig. 7 show the effect of an increasing atmospheric path resulting in greater attenuation at shorter wavelengths. Air-mass values have been assigned for identification purposes and should not be compared to reference spectra or SMARTS. The red curve of Fig. 8 is the measured short circuit current of a multi-junction solar cell in response to the progressively attenuated spectra shown in Fig. 7. The irradiance for the AM 1.5 spectrum was about 42 suns. The modeled air-mass axis of Fig. 8 is not necessarily linear with integrated irradiance; however, as is to be expected, an increase in attenuation results in a decrease in the short-circuit current. The blue curve is the measured current from attenuated spectra which also included the mismatch compensation method that was presented in Fig. 6. Increasing attenuation again reduces the current; however, the measured currents were consistently higher than without compensation because the junction currents are more balanced. The compensated spectra are shown in Fig. 9, where the required amount of compensation was determined by matching to the total integrated irradiance of the modeled air-mass profiles. In the spectral shaper, the amount of compensation was varied by controlling the spectral bandwidth of the compensation light, requiring a wide bandwidth for AM 1.5 and narrower ones for higher air mass.

#### IV. TOWARD HIGHER CONCENTRATION

While the spectral programmability provided by the SLMs is a key feature, their optical loss dramatically reduces the output power of the novel simulator. In the case of the LCOS-SLM, half of the light is lost polarizing the source before the spectral shaper. However, by using a non-programmable simulator with a static amplitude mask [6], we efficiently generated a spectral match to a highly-scaled AM 1.5 reference spectrum, as shown in Fig. 10. Concentrating the static simulator output beam with a parabolic mirror resulted in an irradiance of approximately 570 suns. Fig. 11 shows the measured efficiency curve for a multi-junction solar cell with a short-circuit current (I<sub>sc</sub>) of 10.57 mA, an open circuit voltage (V<sub>oc</sub>) of 3.22 V, and a fill factor of 0.87. The concentrated irradiance in this measurement was more than 4 times higher than the highest irradiance presented in Fig. 3 and Fig. 4, yet the measured short circuit current was only twice as large for the same multi-junction solar cell. This large non-linearity clearly requires further study at intermediary levels of irradiance as well as further consideration of the effects of spectral mismatch below 450 nm. The temperature of the cell, which was not controlled in this work, as well as the pulsed nature of the simulator light at high concentration should also be considered.

Achieving higher irradiance and/or a larger illumination area with our programmable simulator is technically feasible.

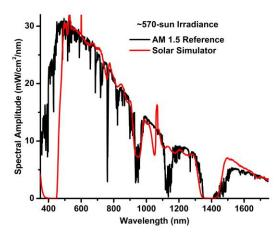


Fig. 10. A concentrated irradiance of approximately 570 suns was achieved with a high efficiency, non-programmable simulator.

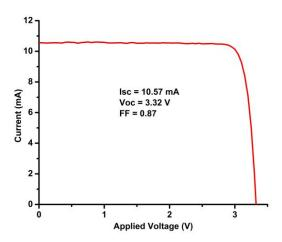


Fig. 11. Measured multi-junction cell efficiency at approximately 570 suns is shown.

For the programmable spectral shaper, a significant increase of more than a factor of two could be realized by replacing the high-loss, polarization selective LCOS-SLM with a long-wavelength optimized GLV-SLM. In addition, supercontinuum lasers having significantly more optical power and spectra which extend down to 400 nm and below are now commercially available. Lasers with ten times as much optical power have been demonstrated in development laboratories and are anticipated to be commercialized in the near future. We estimate that collectively these improvements would allow the programmable simulator to operate at 1000 suns or more over a spot 1 mm in diameter.

## V. CONCLUSION

A super-continuum solar simulator was developed which is capable of creating a high-concentration irradiance appropriate for the characterization of small-area, multi-junction concentrator solar cells. With spectral programmability, the simulator can generate a varying amount of total irradiance as well as realistic spectral variations such as increases in airmass. Using such spectra, variations in multi-junction cell efficiency caused by the imbalance of the individual junction currents can be studied realistically in detail. Future efforts will involve more detailed and quantitative measurements of multi-junction performance based on spectra generated with the SMARTS atmospheric model.

## REFERENCES

- [1] K. Emery, D. Myers, and S. Rummel, "Solar simulation problems and solutions", in *Twentieth PVSC*, Las Vegas, NV, pp. 1087-1091, 1988.
- [2] C. H. Seager, "The determination of grain-boundary recombination rates by scanned spot excitation methods," *J. Appl. Phys.*, vol. 53, no. 8, pp. 5968-5871, 1982.

- [3] B. H. Hamadani, J. Roller, B. Dougherty, and H. Yoon, "Fast and reliable spectral response measurements of PV cells using light emitting diodes," in *Thirty-ninth PVSC*, Tampa, FL, 2013.
- [4] S. R. Kurtz, K. Emery, and J. M. Olson, "Methods for analysis of two-junction, two-terminal photovoltaic devices," in *Proc. World Conf. Photovoltaic Energy Convers.*, Waikoloa, HI, USA, pp. 1733-1737, 1994.
- [5] C. Gueymard, "Parameterized Transmittance Model for Direct Beam and Circumsolar Spectral Irradiance," *Solar Energy*, 71:5, pp. 325-346, 2001.
- [6] T. Dennis, J. B. Schlager, and K. A. Bertness, "A Novel Solar Simulator Based on a Super-Continuum Laser for Solar Cell Device and Materials Characterization," *IEEE J. Photovoltaics*, vol. 4, no. 4, pp. 1119-1127, 2014.
- [7] T. Dennis, "An Arbitrarily Programmable Solar Simulator Based on a Liquid Crystal Spatial Light Modulator," in *Fortieth PVSC*, Denver, CO, pp. 3326 - 3330, 2014.
- [8] D. T. Amm and R. W. Corrigan, "Optical Performance of the Grating Light Valve Technology," in *Proc. SPIE 3634*, *Projection Displays V*, pp. 71-78, 1999.
- [9] Product names are only used in the paper for clarity and do not represent an endorsement by NIST.
- [10] Standard Tables for Reference Solar Spectral Irradiances: Direct Normal and Hemispherical on 37° Tilted Surfaces, G173003, 2008. Available: <a href="http://astm.org">http://astm.org</a>